Swelling Behavior of Cross-Linked Rubber: Explanation of the Elusive Peak in the Swelling Activity Parameter (Dilational Modulus)

ARTICLE *in* MACROMOLECULES · MARCH 2012

Impact Factor: 5.8 · DOI: 10.1021/ma202631u

3 AUTHORS:

Ben Xu
Texas Tech University
10 PUBLICATIONS **48** CITATIONS
SEE PROFILE

Xiaojun Di
Texas Tech University
11 PUBLICATIONS **45** CITATIONS
SEE PROFILE

Gregory B Mckenna
Texas Tech University
334 PUBLICATIONS **8,036** CITATIONS
SEE PROFILE

Macromolecules

Article

pubs.acs.org/Macromolecules

Swelling Behavior of Cross-Linked Rubber: Explanation of the Elusive Peak in the Swelling Activity Parameter (Dilational Modulus)

Ben Xu, Xiaojun Di, and Gregory B. McKenna*

Department of Chemical Engineering, Texas Tech University, Lubbock, Texas 79409-3121, United States

ABSTRACT: There is a considerable body of work in the literature that addresses the swelling of cross-linked rubber in the framework of the Frenkel–Flory–Rehner (FFR) hypothesis that the swelling is controlled by the balance of the thermodynamics of mixing and the elasticity of the network, i.e., the mixing and elastic contributions to the free energy are additive. One outcome that contradicts the FFR hypothesis of the experimental aspects of the work is that the swelling activity parameter (or dilational modulus) $S = \lambda \ln(a_c/a_u)$ frequently shows a peak when plotted as a function of the swelling stretch λ_s^2. a_c and a_u are the chemical potentials of cross-linked and un-cross-linked rubber at fixed polymer volume fraction. The focus of the present work is the behavior of S, which has remained elusive of explanation, and that we propose is an artifact of the data treatment used in the determination of the value of S as a function of λ_s^2. This is because the data treatment generally has required curve smoothing of (generally) sparse experimental data for swelling of the rubber as a function of the chemical activity and, then, taking the logarithm of the ratio of a_c/a_u at fixed volume of polymer in the system. We find that the peak in S disappears when using a model based smoothing method instead of the empirical or polynomial methods of smoothing the individual volume fraction vs chemical activity curves for the cross-linked and un-cross-linked rubbers. We propose that the "peak" in S is due to the experimental variability in sparse data and is emphasized in the common methods of data smoothing. We show that addition of less than 1% random error to the model data can lead to the peak in S. Importantly, this work shows that the Frenkel–Flory–Rehner theory is consistent with the swelling data and the elusive peak in S is actually an artifact of normal data smoothing procedures.

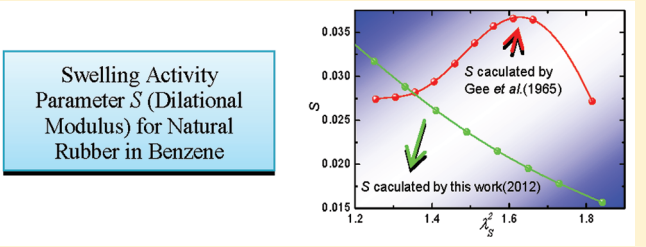

1. INTRODUCTION

The present story began in 1965, when Gee, Herbert, and Roberts[1] observed that for natural rubber in benzene, the swelling activity parameter S, first defined in the context of the Frenkel[2]–Flory–Rehner[3] (FFR) hypothesis and also referred to as the "dilational modulus",[4] went through a maximum as swelling stretch λ_s^2 increased in isopiestic vapor sorption experiments as shown in Figure 1a. This phenomenon cannot be explained by the FFR hypothesis, which provides the fundamental underpinning of swelling behavior and an explanation continues to be elusive. The existence of the peak is very important to our understanding of the thermodynamics of networks, i.e., is the FFR hypothesis correct or not? Furthermore, this ambiguous behavior of S would also suggest that the presence of solvent possibly affects the entropy of mixing and/or elasticity of the network. For example, Eichinger and co-workers[4−11] conducted a series of experiments on styrene–butadiene rubber (SBR) and poly(dimethylsiloxane) (PDMS) rubber swollen in different solvents and tried to use their model to "capture" the "peak" in S. However, the model used does not correctly describe the behavior of S, with especially large deviations observed in the low λ_s^2 region. The data also seemed to show somewhat erratic results in the appearance of the "peak" in S with a consequence of no particular trend in S with, e.g., solvent quality. Gottlieb and Gaylord examined the ability of nine different rubber elasticity models (elastic free energy form differed) to describe the unexplained "peak" in S.[12] They found that only four of the models can even qualitatively agree with the data for S obtained by Eichinger et al.[5−7,11] and Roberts et al.[1] One of these four models cannot describe the experimental data quantitatively while the other three can give quantitative agreement with the "peak", only if the fitting parameters used in the rubber elasticity models have unphysical values. Gottlieb and Gaylord speculated that this was because none of these molecular theories were developed enough or that there could be something wrong in the FFR hypothesis. Gottlieb and co-workers[13] also proposed a less complicated model in which it was assumed that S depended on the solvent quality. This also did not succeed in describing reported behaviors. Deloche and Samulski[14] proposed a model that considered the segment–segment (and segment-solvent) orientational/relationships, which come from the stretching of chains in the swollen network, with the aim of interpreting the appearance of a solvent-dependent maximum in S but still could not find the rule of the "peak". McKenna and Crissman[15] systematically studied the connection between the "peak" with cross-linking density and temperature in a polyisoprene cross-linked by

Received: December 7, 2011
Revised: January 25, 2012
Published: February 17, 2012

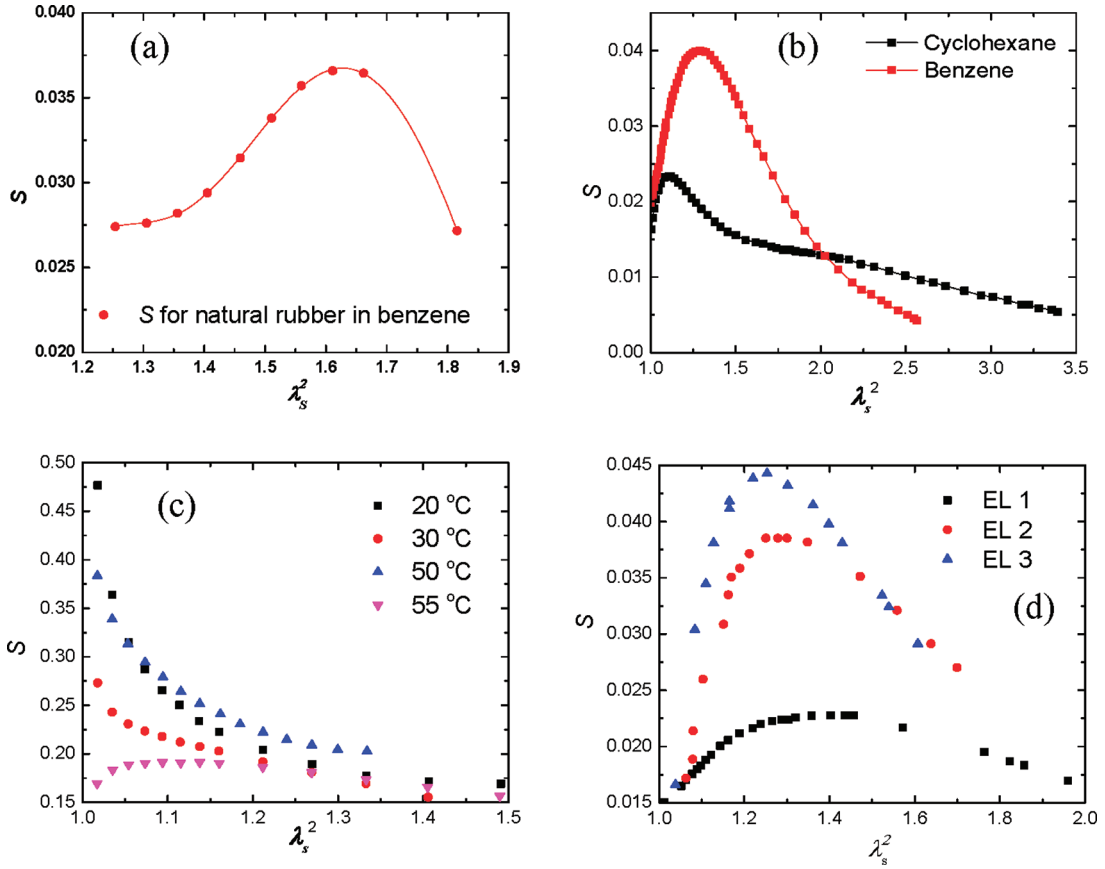

Figure 1. (a) *S* for cross-linked natural rubber swollen in benzene vapor at 25 °C obtained by Gee et al.[1] (b). *S* for PDMS in benzene and cyclohexane vapors at 30 °C[7] (c) *S* for 15 phr dicumyl peroxide cross-linked polyisoprene in benzene vapor at 20 °C, 30 °C, 50 and 55 °C.[15] (d) *S* for different cross-linking density PDMS in cyclohexane at 30 °C.[5]

different amounts of dicumyl peroxide. They found the appearance of the "peak" varies dramatically with temperature or cross-linking density and they speculated that it may be due to some unspecified special solvent−polymer interaction. Nandi and Winter[16] proposed that this ambiguous behavior in *S* may be due to a specific solvent effect because the work had only considered relatively few solvents. They also pointed out that Russ et al.[17] studied the swelling of a network in a polymeric solvent and no peak was observed, indicating that the FFR hypothesis is valid in the macromolecular solvent. Indeed, *S* might show a different dependence in the polymeric solvent, but the statement that the ambiguous *S* behavior is solvent dependent cannot be concluded from Russ et al.'s paper.[17]

In sum, many researchers have been interested in the origins of the peak in *S*, but a full explanation of *S* has remained elusive.[1,4−18] The lack of explanation for the "peak" in *S* has also resulted in questions related to the validity of the FFR hypothesis that the elastic and mixing parts of the Helmholtz free energy in swollen rubber networks are separable and additive.[4−11,15,19]

In the present paper, we show for the first time that the appearance of the peak in *S* is rooted in artifacts that arise from the smoothing procedures used for relatively sparse experimental data for volume fraction of polymer as a function of chemical potential. Previously, polynomial smoothing or "empirical smoothing[1]" methods were used to smooth the curves of isopiestic vapor sorption data and the *S* was calculated from the smoothed data.[1,4−11,15] Here we discuss and compare the results of *S* obtained by different smoothing methods to show that the "peak" in *S* may occur simply because the experimental uncertainty is magnified by the smoothing method. The data we analyze in this paper come from isopiestic vapor sorption experiments[15] (to determine *S*) and torsional experiments (to determine the elastic contribution to the Helmholtz free energy) from the literature.[20]

2. METHODOLOGY

2.1. The Origin of the *S* Problem. The FFR hypothesis states that the mixing and the elastic contributions to the free energy are additive and equal in swelling equilibrium, which is usually written in terms of the chemical potential difference between the rubber-solvent system and the pure solvent as[3,21−23]

$$(\mu_1 - \mu_1^0)_{mix} = -(\mu_1 - \mu_1^0)_{el} \quad (1)$$

It is generally accepted that the mixing term in the Flory[24]−Huggins[25] expression is

$$(\mu_1 - \mu_1^0)_{mix} = RT[\ln(1 - \nu_2) + \nu_2 + \chi\nu_2^2] \quad (2)$$

where ν_2 is the volume fraction of the rubber, χ is the Flory[24]−Huggins[25] interaction parameter. The elastic contribution to the chemical potential can be expressed in terms of the Valanis−Landel[26] function:

$$(\mu_1 - \mu_1^0)_{el} = V_1 w'(\lambda)/RT\lambda^2 \quad (3)$$

The FFR hypothesis can explain most of the problems in swelling when handled properly[27−31]with the exception of the

dx.doi.org/10.1021/ma202631u | *Macromolecules* 2012, 45, 2402−2410

swelling activity parameter S.[15] S, representing a difference in free energy between the cross-linked and the un-cross-linked systems, is defined in the context of the FFR hypothesis as[15]

$$S = \lambda \ln(a_c/a_u) \tag{4}$$

$$\lambda = {\nu_2}^{-1/3} \tag{5}$$

$$\ln(a_u) = [\ln(1 - \nu_2) + \nu_2 + \chi_u {\nu_2}^2] \tag{6}$$

$$\ln(a_c) = [\ln(1 - \nu_2) + \nu_2 + \chi_c {\nu_2}^2] + V_1 w'(\lambda)/RT\lambda^2 \tag{7}$$

where a is the solvent activity. In this paper, a is defined as $a = P/P_0$ where P = pressure and P_0 = saturation vapor pressure. The subscripts u and c refer to the un-cross-linked and the cross-linked rubbers, respectively. V_1 is the molar volume of the solvent, R is the gas constant, w is the elastic contribution to the Helmholtz free energy and interpreted in the continuum sense of a Valanis–Landel model or hyperelastic materials.[26] w' is the derivative of w with respect to the stretch λ, and w is the strain energy density function of the elastic network.

The data plots of ν_2 vs a_c and a_u are generally obtained from isobaric vapor sorption experiments as shown in Figure 2. As

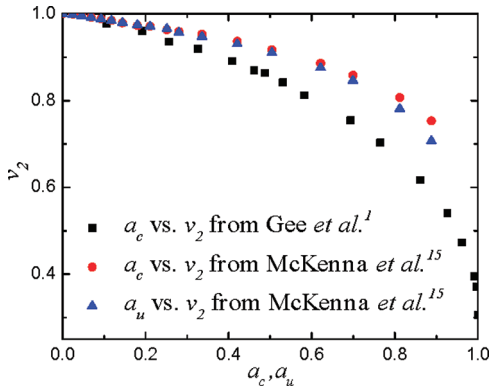

Figure 2. Isopiestic vapor sorption experimental data[1,15] illustrating that the density of points is sparse.

seen in Figure 2 and detailed subsequently, the data are relatively sparse. For the past half century, polynomial smoothing or "empirical smoothing[1]" methods were used to smooth this sparse data of ν_2 vs a or P to obtain values of a_c and a_u at the corresponding fixed ν_2 and substitute into eq 4 to calculate S.[1,4−10,14] Previous researchers have performed much work to explore the rule of S. There, strange "peaks" in S vs λ_s^2 curves, as illustrated Figure 1, have been reported to depend on solvent[7] (Figure 1b), temperature[15](Figure 1c), cross-linking density[8] (Figure 1d), and have been interpreted to contradict the FFR hypothesis. Some mathematical models and modified theories were developed to capture the "peaks" but none of them give satisfying results. As described in the Introduction, because no general rules have been concluded from the existence of the peak in S, some researchers have speculated that there might be some unknown special interaction between the solvent and the rubber.[15] However, no one has previously questioned the validity of the data smoothing procedures used to treat the swelling data and to calculate the value of S at the different values of polymer network volume fractions.

We hypothesize that this sparse experimental data causes the smoothing methods used for interpolation of the data to magnify the experimental uncertainties and, consequently, produce the ambiguous peaks in S. In order to test this assumption, we used the FFR model in analytical form, added random error to the model data to construct simulated experimental data, and then two different polynomial fitting methods were used to smooth the data. From these results we find that even a small amount of random error (<1%) can induce a peak in S. Furthermore, because error added to the smoothed data differ for each run of the computer program, the peak in S shows a different shape for each run even for the same percent of random error. We also produced simulated experimental data with different data densities or sparseness and show that this also influences the peak in S even though the underlying model is smooth and does not give a peak.

2.2.1. Methods. *Polynomial Smoothing.* For the past half century, polynomial smoothing or "empirical smoothing[1]" methods have been used to smooth the data of a or P vs ν_2 to calculate S.[1,4−11,15] For the purpose of comparison, in this paper, we used third-order and fourth-order polynomials to smooth the data plots of a vs ν_2 for both cross-linked and un-cross-linked rubbers. The obtained a_c and a_u as functions of ν_2 were then used to calculate S from eq 4.

2.2.2. FFR smoothing. We generated the FFR smoothing method from the definition of S and the Flory–Huggins equation.

$$\chi_c = \nu_2 \chi_{c0} + \chi_{c1} \tag{8}$$

$$\chi_u = \nu_2 \chi_{u0} + \chi_{u1} \tag{9}$$

$$\ln(a_u) = [\ln(1 - \nu_2) + \nu_2 + \chi_{u0} {\nu_2}^3 + \chi_{u1} {\nu_2}^2] \tag{10}$$

$$\ln(a_c) = [\ln(1 - \nu_2) + \nu_2 + \chi_{c0} {\nu_2}^3 + \chi_{c1} {\nu_2}^2] + V_1 w'(\lambda)/RT\lambda^2 \tag{11}$$

In the FFR model, we substitute eqs 8 and 9 into eqs 6 and 7 to make χ_c and χ_u polymer volume fraction ν_2 dependent as shown in eqs 10 and 11. Subsequently eqs 10 and 11 were used to smooth the data of a vs ν_2 with χ_{c0}, χ_{c1}, χ_{u0} and χ_{u1} being fitting parameters. The elasticity contribution in eq 11 was calculated from torsional data using the constrained chain model[32−38] as detailed in section 3.1.

Table 1. Equations and Fitting Parameters Used for the Three Smoothing Methods

method	equations relating ac and au vs ν_2	physical meaning	fitting parameters	elasticity
1	3rd-order polynomial	no	ν_2, a_c, a_u	no
2	4th-order polynomial	no	ν_2, a_c, a_u	no
3	FFR smoothing function, eqs 8−11	yes	χ_{c0}, χ_{c1}, χ_{u1}, χ_{u1}	yes

3. RESULTS AND DISCUSSION

Although results for S have been reported on many occasions,[1,4−11,15] few works show the original data. Rather they only report the smoothed curves. Also most researchers did not consider the contribution of the elasticity to S except for the works of McKenna and his co-workers.[15,20,27−30,34] In the present paper, we have primarily reanalyzed the isopiestic

dx.doi.org/10.1021/ma202631u | *Macromolecules* 2012, 45, 2402−2410

vapor sorption experiments conducted by McKenna and Crissman[15] and used the torsional data obtained by McKenna et al.[20] to determine the elastic contribution to the Helmholtz free energy.

3.1. Calculation of the Elasticity Contribution. According to the definition of S in the context of the FFR hypothesis, not only the mixing free energy contributes to S but also the elastic free energy. In this paper, the contribution of the elasticity $V_1w'(\lambda)/RT\lambda^2$ was calculated from the torsional measurements on dicumyl peroxide cross-linked polyisoprene conducted by McKenna et al.[20] The samples were designated by the amount of dicumyl peroxide from one part peroxide per hundred parts rubber (phr) to 15 phr. We calculated $V_1w'(\lambda)/RT\lambda^2$ from $w'(\lambda) - ((w'(1))/(\lambda))$ from the constrained chain model[32−38] fit to the data of $w'(\lambda) - ((w'(1))/(\lambda))$ vs λ. The constrained chain model has been shown to give a reasonable fit to the network elasticity by Han et al.[36] The stain energy function derivative is expressed in terms of the derivative of elastic free energy[20,27−30,36] through the Valanis−Landel function:[26]

$$\frac{\partial \Delta F_{el}}{\partial \lambda} = w'(\lambda) - \frac{w'(1)}{\lambda} \tag{12}$$

The elastic free energy is given by[32,33,36]

$$\Delta F_{el} = \Delta F_{el}^{c} + \Delta F_{el}^{ph} \tag{13}$$

where ΔF_{el}^{ph} is the elastic free energy of deformation by the phantom model, which is given by

$$\frac{\Delta F_{el}^{ph}}{kT} = \left(\frac{\xi}{2V_0}\right)(\lambda_1^2 + \lambda_2^2 + \lambda_3^2 - 3) \tag{14}$$

ΔF_{el}^{c} is the contribution arising from entanglement constraints relative to those in the phantom network, which can be written[34−38]

$$\Delta F_{el}^{c} = \frac{1}{2}\xi kT \sum_i \left\{\lambda_i^2 - 1 + \left(\frac{\nu_{el}}{\xi}\right)[B_i + D_i - \ln(1 + B_i) - \ln(1 + D_i)]\right\} \tag{15}$$

where

$$h(\lambda_i) = \kappa_G\left[1 + \frac{(\lambda_i^2 - 1)\left(1 - \frac{2}{f}\right)^{2/3}}{3}\right] \tag{16}$$

$$B_i = \frac{h(\lambda_i)\kappa_G\left[1 - \left(1 - \frac{2}{f}\right)^{2/3}\right](\lambda_i^2 - 1)}{[\lambda_i^2 + h(\lambda_i)]^2} \tag{17}$$

$$D_i = \frac{\lambda_i^2 B_i}{h(\lambda_i)} \tag{18}$$

$$\dot{B}_i = \frac{\partial B_i}{\partial \lambda} \tag{19}$$

$$\dot{B}_i = B_i\left\{\frac{1}{\lambda_i^2 - 1} - \frac{2}{\lambda_i^2 + h(\lambda_i)}\right\} + \frac{\kappa_G[\lambda_i^2 + h(\lambda_i)]\left(1 - \frac{2}{f}\right)^{2/3}}{h(\lambda_i)[\lambda_i^2 + h(\lambda_i)]} \tag{20}$$

$$\dot{D}_i = \frac{\partial D_i}{\partial \lambda} \tag{21}$$

$$\dot{D}_i = B_i\left[h(\lambda_i)^{-1} - \frac{\lambda_i^2\kappa_G\left(1 - \frac{2}{f}\right)^{2/3}}{h(\lambda_i)^2}\right] + \frac{\lambda_i^2\dot{B}_i}{h(\lambda_i)} \tag{22}$$

where f is the functionality of the network junctions, ξ is the cycle rank of the network, k is the Boltzmann constant and T is the absolute temperature.ξ,κ_G and ν_{el} are the fitting parameters. The constrained chain model[32−38] fit to the torsional measurement data for the 10 phr cross-linked rubber (data from McKenna et al.[20]) is shown in Figure 3. We extrapolate

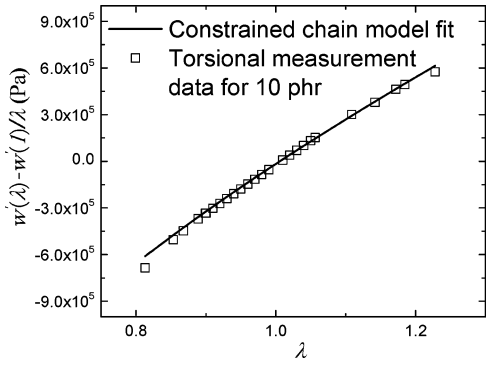

Figure 3. Constrained chain model[32−38] fit to the torsional measurement data for the 10 phr cross-linked rubber (data from McKenna et al.[20]).

the value of $w'(\lambda) - ((w'(1))/(\lambda))$ in the range of λ = 1−1.24 from the constrained chain model[32−38] fit to calculate $V_1w'(\lambda)/RT\lambda^2$.

Figure 4 shows the results of $V_1w'(\lambda)/RT\lambda^2$vs λ for the 1 phr, the 5 phr, and the 15 phr cross-linked rubber, from which it can be concluded that the higher the cross-linking density, the stronger the dependence of $V_1w'(\lambda)/RT\lambda^2$on λ, similar to the dependence of $w'(\lambda) - ((w'(1))/(\lambda))$ on λ.[27−30]

3.2.1. Results of *S*. *Smoothing of the Experimental Data of ν_2, vs a.* The volume fractions ν_2 of an un-cross-linked natural rubber and the 15 phr cross-linked rubber vs a at 55 °C in benzene vapor are shown in Figure 5 along with curves from third-order polynomial smoothing, fourth-order polynomial smoothing and FFR model smoothing. As seen from eq 4, in order to calculate S, the values of a_c and a_u at the same ν_2 must be known. Yet, in the experimental data, only a_c and a_u at different ν_2 are generally obtained. Therefore, the experimental data for ν_2 vs a_c and a_u were smoothed to get obtain fitting parameters that were used to calculate the values of a_c and a_u at the same values of ν_2. These were then substituted into eq 4 to calculate S. Prior researchers[1,4−11,15] used polynomial or "empirical smoothing" methods to smooth the isopiestic

dx.doi.org/10.1021/ma202631u | Macromolecules 2012, 45, 2402−2410

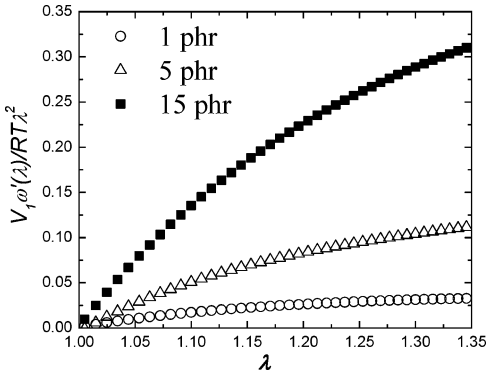

Figure 4. $V_1w'(\lambda)/RT\lambda^2$ vs λ for the 1 phr, the 5 phr, and the 15 phr cross-linked rubber. (Calculated from the data obtained by McKenna et al.[20]).

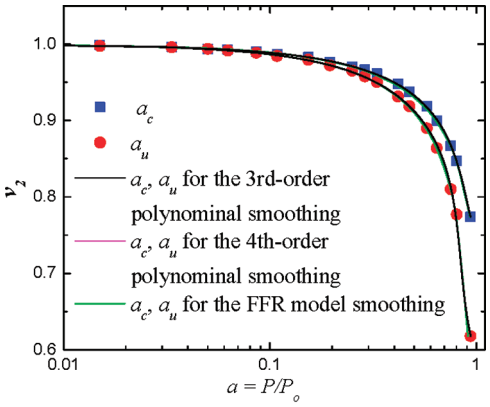

Figure 5. a vs v_2 for the 15 phr cross-linked rubber in benzene vapor at 55 °C along with the third-order polynomial smoothing, the fourth-order polynomial smoothing and the FFR model smoothing. (Data come from McKenna and Crissman.[15])

vapor sorption experimental data. As shown in Figure 5, the experimental data is relatively sparse, and the polynomial smoothing, is more likely to have slight "wiggles" that, consequently, magnify the experimental uncertainties when calculating S. It cannot be told which method is better from Figure 5, which is another reason why previous researchers did not question the validity of the polynomial smoothing procedure. However, the values of S calculated from the different smoothing methods show dramatic differences as shown in Figure 6 and discussed next.

3.2.2. Comparison of S Obtained by Different Smoothing Procedures. Figure 6 presents S vs λ_s^2 calculated by different smoothing methods for the 10 phr cross-linked rubber at 50 °C in the benzene vapor. The "peak" appears in the results obtained using the polynomial smoothing. The shape and the position of the peaks vary for the results produced by the third-order and fourth-order polynomial smoothing to the isopiestic data, indicating that the polynomial seems to introduce the peak. The S vs λ_s^2 results obtained by the FFR model smoothing, as expected, do not show any peak and their shapes are consistent with the FFR hypothesis.

For Eichinger's PDMS results,[5,7] S is 10 times smaller than the value of S in polyisoprene reported by McKenna and Crissman.[15] This is because the elastic contribution to S of PDMS is only one-quarter that of the polyisoprene and this leads to smaller differences in the vapor sorption of cross-linked and un-cross-linked PDMS and therefore smaller values of S.

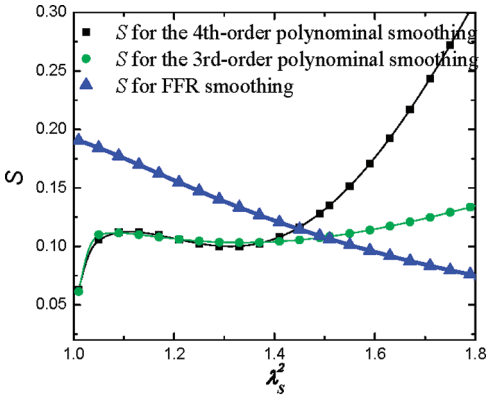

Figure 6. Comparison of S for the 10 phr cross-linked rubber at 50 °C in benzene vapor obtained by different smoothing methods: third-order polynomial smoothing, fourth-order polynomial smoothing and FFR model smoothing. (Data from McKenna and Crissman.[15])

We also recalculated the "classic peak" of Gee et al.[1] As shown in Figure 7, in the results obtained by the FFR

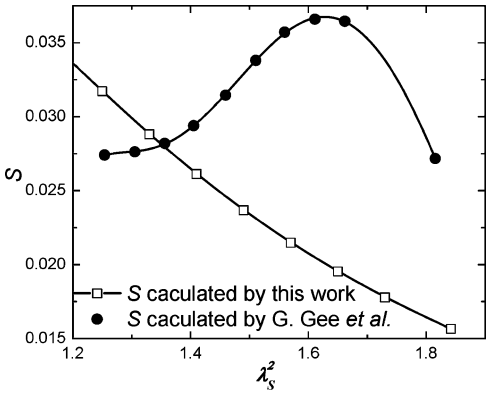

Figure 7. Comparison of S obtained by different methods. (Data from Gee et al.[1])

smoothing, the peak disappears and the behavior of S is, then, consistent with the FFR hypothesis. After dealing with the isopiestic vapor sorption data for different rubbers in different environments (the 1 phr, the 5 phr, the 10 phr, and the 15 phr cross-linked rubber in benzene at 10−55 °C,[15]) we found that the "peak" only appears in the S vs λ_s^2 plots obtained when using polynomial smoothing or from "empirical smoothing[1]". Since the peak is not inherent to the FFR hypothesis, this leads to a question: Is the "peak" researchers have been trying to understand simply an artifact of the data smoothing procedure and, consequently, does not lead to a need to replace the FFR hypothesis?

4. HOW TO PRODUCE THE "PEAK" IN S

In order to further explore the nature of the "peak" in S and to make comparisons with different smoothing methods, we carried out a study using model data. We used the FFR model, which does not inherently show a peak, as a model function to which noise was added. n points in v_2 with the same range as the experimental data shown previously were selected and the corresponding activities from the above analytical functions (eqs 4−7) were calculated as shown schematically in Scheme 1. The model values chosen were those we obtained by smoothing the data using the FFR model above. The elasticity

dx.doi.org/10.1021/ma202631u | *Macromolecules* 2012, 45, 2402−2410

Scheme 1. Schematic of Procedure To Test Whether Peak in *S* Is Caused by the Polynomial Data Smoothing

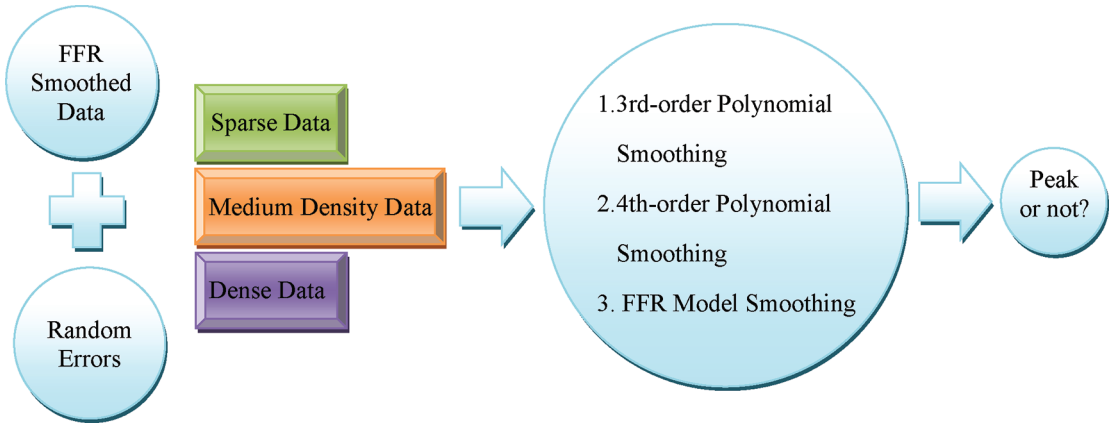

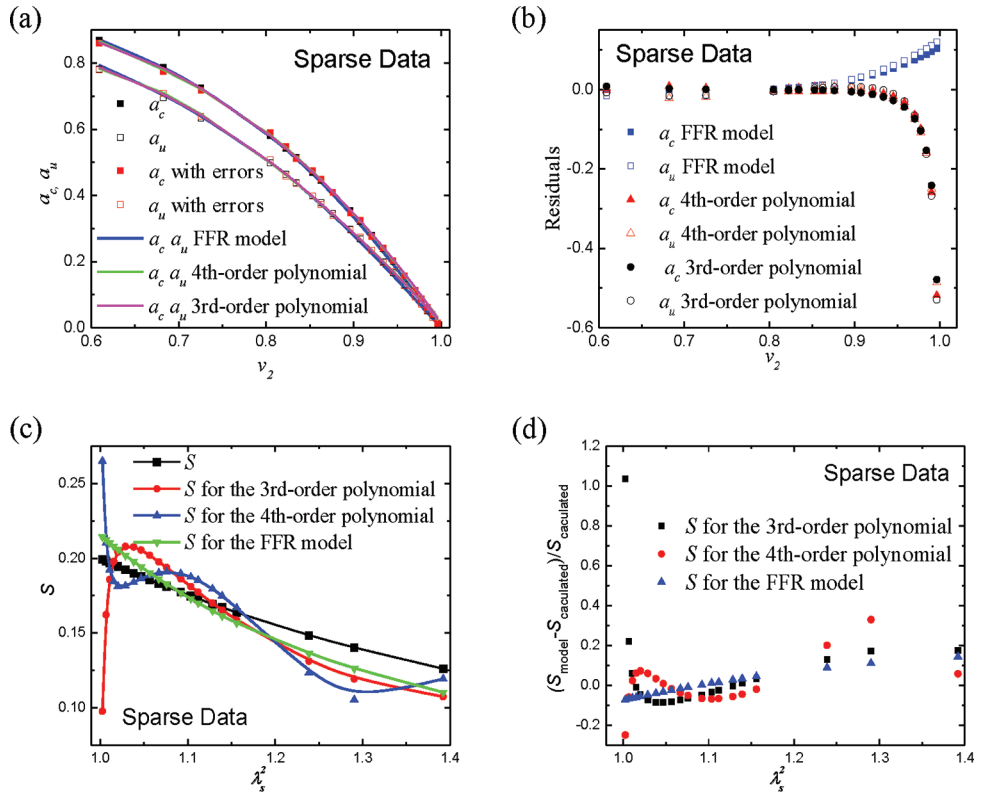

Figure 8. One example of the results of the sparse data (20 points) obtained by the Matlab[39] program (with error limits of 2%). The FFR model, third-order polynomial and fourth-order polynomial to the sparse simulated experiment data: (a) a vs v_2; (b) residuals $((a - a_{fit})/(a_{fit}))$ vs v_2; (c) S for the third-order polynomial, fourth-order polynomial, and the FFR model along with the sparse "simulated" experimental data; (d) $(s_{model} - s_{calculated})/(s_{calculated})$.

contribution was calculated from the fit of the constrained chain model[32−38] to the torsional experiments. The model data are designated as $(v_{21}, a_{u1\_model}, a_{c1\_model})$, $(v_{22}, a_{u2\_model}, a_{c2\_model})$, $(-\cdots\cdots-)$ $(v_{2n}, a_{un\_model}, a_{cn\_model})$. A Matlab[39] program was written and added noise $N(v_2)$ to the FFR function model data using the following expressions

$$N(v_2) = 1 + 2 \times (\text{rand} - 0.5) \times P \tag{23}$$

$$a_{c\cdot simulated} = a_{c\cdot model} \times N(v_2) \tag{24}$$

$$a_{u\cdot simulated} = a_{u\cdot model} \times N(v_2) \tag{25}$$

where P is the percent of the random error limits and rand is a random number range from 0−1 picked up by the Matlab[39] program. The random error added to the model data are different for each run of the program but do not exceed the random error limit P. Subsequently, different smoothing methods were used to smooth the simulated experimental data $((v_{21}, a_{u1\_simulate}, a_{c1\_simulate}), (v_{22}, a_{u2\_simulate}, a_{c2\_simulate}), \ldots, (v_{2n}, a_{un\_simulate}, a_{cn\_simulate}))$ to calculate S in order to test how big the error needs to be to induce the "peak" in S.

As mentioned previously, the sparse data also triggers the polynomial to magnify the experimental uncertainties. Here we have compared the results obtained using the polynomial for the simulated data having different data densities: 1. set the

dx.doi.org/10.1021/ma202631u | *Macromolecules* 2012, 45, 2402−2410

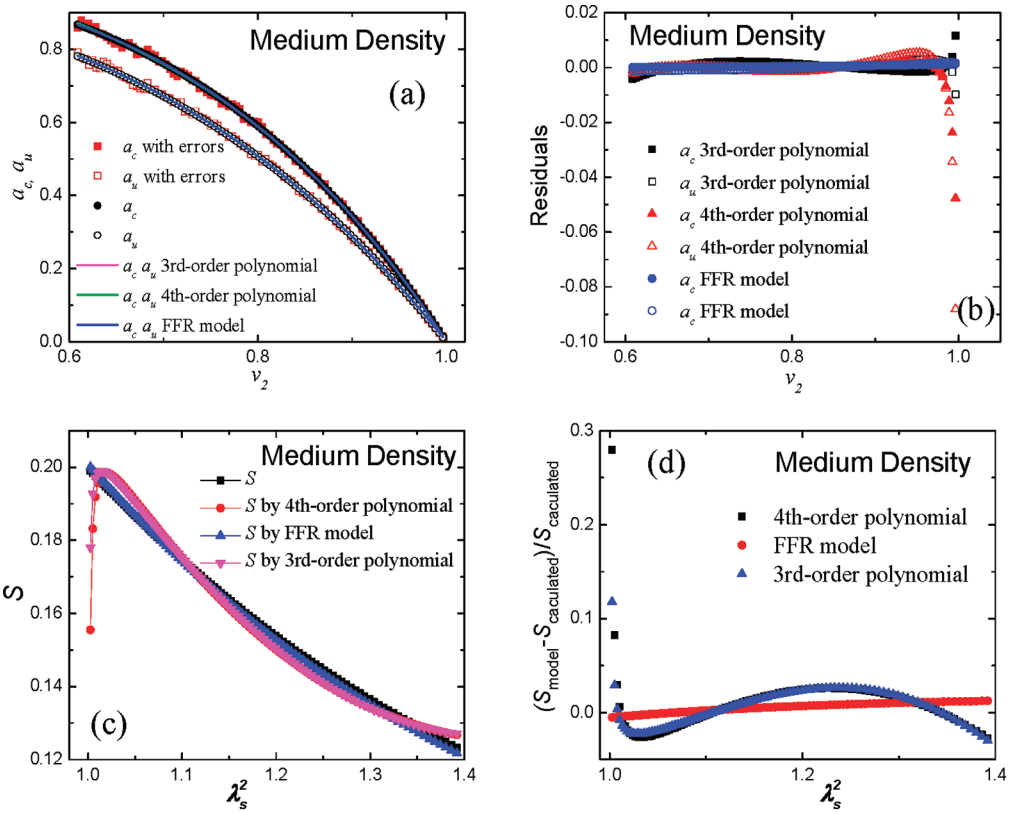

Figure 9. One example of the results of the medium density data (100 points) obtained by the Matlab[39] program (with error limits of 2%). The FFR model, the third-order polynomial, and the fourth-order polynomial to the medium density simulated experiment data: (a) a vs ν_2; (b) residuals $((a - a_{fit})/(a_{fit}))$ vs ν_2; (c) S for the third-order polynomial, fourth-order polynomial, and the FFR model along with the medium density "simulated" experimental data; (d) $(s_{model} - s_{calculated})/(s_{calculated})$

number of the model data n to be the number of the experimental data to make sparse data. 2. Generate 5× the number of the experimental data to make medium-density simulation data. 3. Generate 50× experimental data to make dense simulation data.

Here we present the results obtained by the third-order and the fourth-order polynomial methods. We also used the FFR model to smooth the sparse, medium densities, and dense simulated experimental data generated for the value of a_c and a_u vs ν_2 for polyisoprene and the 10 phr cross-linked rubber at 50 °C. The errors are random so different results will be found for each run and we only show typical representative results.

A set of typical simulated results (with error limits of 2%) are displayed in Figure 8 (sparse data) and Figure 9 (medium density data) and Figure 10 (dense data). Looking first at the sparse data of Figure 8, it cannot be told which method is better from Figure 8a, which may be the reason why the validity of the polynomial smoothing has not been generally questioned. However, as shown in Figure 8b, the residuals of the FFR smoothing are much smaller than the third and fourth-order polynomial smoothing, indicating the FFR model describes the experimental data better. As displayed in Figure 8b, large residuals from the polynomial are observed at ν_2 close to 1, which is also the range where the peak often appears. Figure 8c compares the "real value" of S (calculated from the simulated experimental data directly) and the S obtained for the FFR model smoothing and the polynomial smoothing. Peaks at small λ_s^2 (large ν_2) are observed in the results from the third-order and fourth-order polynomial smoothing, which strongly suggests that the appearance of the mysterious peak in S is rooted in the way in which the experimental uncertainty is emphasized by the polynomial or empirical data smoothing methods. Figure 8d shows the error between the model calculated data (error free) S and the third-order, the fourth-order polynomial and the FFR smoothing procedures. It can be seen that the FFR smoothing gives results that do not have the artifacts that seem to be introduced by the polynomial methods. More importantly, the results displayed in Figure 8–10 are from a single run of the model plus error. Because the errors added in the original data are random (the only constraint here is the error limits), the figures look different for each run (set of random errors).

However, some general points can be concluded from the sparse-data simulation. (1) When the added error limit is smaller than 0.2%, the differences between the results obtained by the polynomial and the FFR model are small and no peaks are observed. The bigger the added error limit, the bigger the difference between the results obtained by the polynomial and the FFR smoothing procedures. When the added error is larger than 0.5%, the "peak" produced by the polynomial method becomes notable. (2) When the added error limit is larger than 1%, the shape of the S from the polynomial smoothing shows dramatic differences for each run and the "peak" becomes prominent, because errors added are random and the polynomial is more likely to exaggerate the introduced uncertainties. The "peaks" produced by our program are similar to those reported in the literature. (3) The S obtained by the FFR model does not produce a "peak" and is consistent with the FFR hypothesis if we accept that $\chi_c > \chi_u$. From Figure 9, parts b and d, we can see that the FFR model can always fit

dx.doi.org/10.1021/ma202631u | Macromolecules 2012, 45, 2402–2410

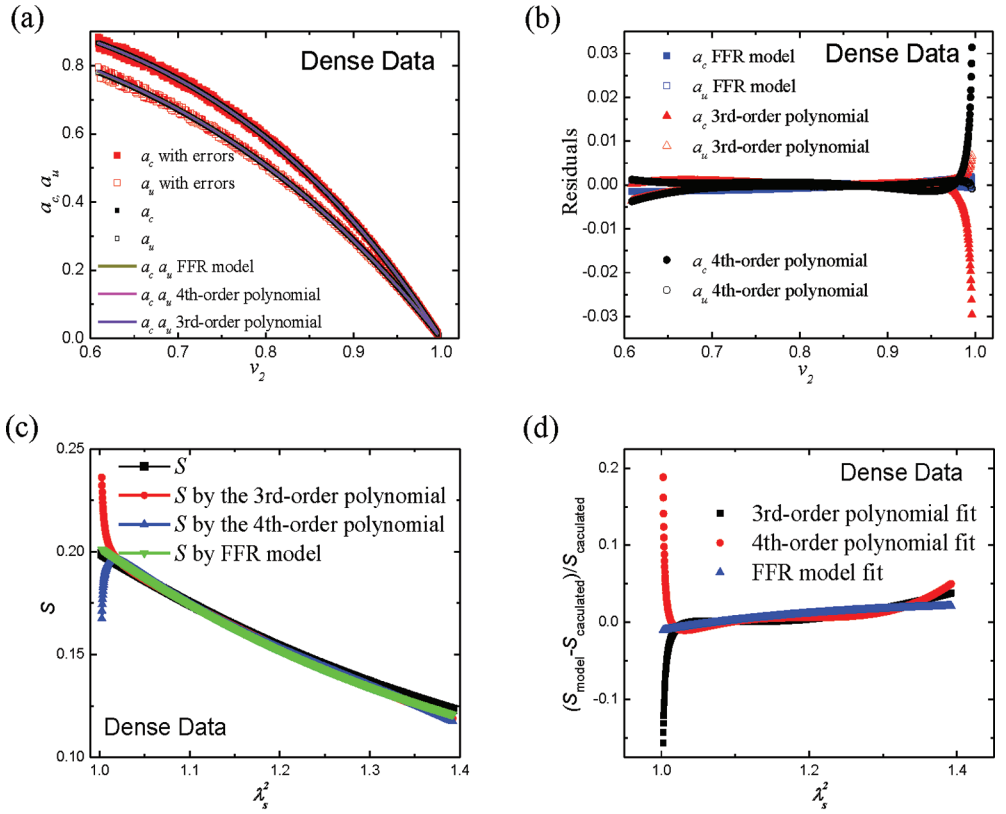

Figure 10. One example of the results of dense data (1000points) obtained by the Matlab[39] program (with error limits of 2%) The FFR model, the third-order polynomial, and the fourth-order polynomial to the dense simulated experiment data: (a) a vs v_2; (b) $(a_{c\ by\ polynomil\ fit})/(a_c)$, $(a_{u\ by\ polynomil\ fit})/(a_u)$, $(a_{c\ by\ the\ FFRmodel\ fit})/(a_c)$, $(a_{u\ by\ the\ FFRmodel\ fit})/(a_u)$); (c) S for the third-order polynomial, fourth-order polynomial and the FFR model along with the dense "simulated" experimental data; (d). $(s_{model} - s_{calculated})/(s_{calculated})$.

the simulated experimental data better than the polynomial. There are some differences for each run of the results obtained by the FFR smoothing method when the added error is larger than 1% but the results maintain a similar shape and trend which distinguish it from the polynomial smoothing.

If we compare the results from Figures 8−10, several conclusions can be made: (1) The denser the data, the less ambiguous is S and smaller errors are introduced by the polynomial smoothing. In the dense simulated results treated by polynomial smoothing, there can still be some bump in S in the region of v_2 near 1, which is because the value of mass uptake is very small and the result is more sensitive in this region. (2) The sparse data collection generally used in the isopiestic vapor sorption experiments is another cause of the ambiguous peak in S produced by the polynomial smoothing.

From the analysis above, it can be concluded that the ambiguous "peak" in S is simply a misconception engendered by experimental uncertainties magnified by the data smoothing methods, e.g. polynomial smoothing or "empirical smoothing[1]".

5. CONCLUSIONS

By comparing the results of swelling activity parameter S obtained by different data smoothing methods, we have shown that the "peak" in S that has puzzled the polymer physics community for a half century, is an artifact rooted in experimental uncertainty of sparse data that is magnified by conventional smoothing methods (polynomial smoothing and "empirical smoothing"). To test this hypothesis, we added random error to a model of the thermodynamics of swelling to create simulated experimental data and compared the values of S obtained by different smoothing methods to the simulated experimental data. It results that the polynomial smoothing of data, with as little as 0.5% random error added, causes the appearance of peaks in S which confirms the hypothesis and shows that the S is a monotonic function of swelling and the apparent peaks that have been reported in S are artifacts of the data treatment and not evidence of the breakdown of the Frenkel-Flory−Rehner theory of network swelling.

AUTHOR INFORMATION

Corresponding Author

*E-mail: greg.mckenna@ttu.edu..

Notes

The authors declare no competing financial interest.

ACKNOWLEDGMENTS

The authors are grateful to the Office of Naval Research (ONR) under Project Nos. N00014−06−1−0922, N00014−11−1−0424 and the John R.Bradford endowment at Texas Tech University for partial supportof this work.

REFERENCES

(1) Gee, G.; Herbert, J. B. M.; Roberts, R. C. *Polymer* **1965**, *6*, 541.
(2) Frenkel, J. *Acta. Phys. USSR* **1938**, *9*, 235; *Rubber Chem. Technol.* **1940**, *13*, 264.
(3) Flory, P. J.; Rehner, J. J. Jr. *J. Chem. Phys.* **1943**, *11*, 521.
(4) Neuburger, N. A.; Eichinger, B. E. *Macromolecules* **1988**, *21*, 3060.
(5) Brotzman, R. W.; Eichinger, B. E. *Macromolecules* **1983**, *16*, 1131.
(6) Brotzman, R. W.; Eichinger, B. E. *Macromolecules* **1981**, *14*, 1445.
(7) Brotzman, R. W.; Eichinger, B. E. *Macromolecules* **1982**, *15*, 531.

(8) Zhao, Y. Q.; Eichinger, B. E. *Macromolecules* **1992**, *25*, 6988.
(9) Zhao, Y. Q.; Eichinger, B. E. *Macromolecules* **1992**, *25*, 6996.
(10) Yen, L. Y.; Eichinger, B. E. *J. Polym. Sci., Part B: Polym. Phys.* **1978**, *16*, 117.
(11) Yen, L. Y.; Eichinger, B. E. *J. Polym. Sci., Part B: Polym. Phys.* **1978**, *16*, 121.
(12) Gottlieb, M.; Gaylord, R. J. *Macromolecules* **1984**, *17*, 2024.
(13) Pekarski, P.; Rabin, Y.; Gottlieb, M. *J. Phys. II Fr.* **1994**, *4*, 1677.
(14) Deloche, B.; Samulski, E. T. *Macromolecules* **1988**, *21*, 3107.
(15) McKenna, G. B.; Crissman, J. M. *J. Polym. Sci., Part B: Polym. Phys.* **1997**, *35*, 817.
(16) Nandi, S.; Winter, H. H. *Macromolecules* **2005**, *38*, 4447.
(17) Russ, T.; Brenn, R.; Geoghegan, M. *Macromolecules* **2003**, *36*, 127.
(18) Horta, A.; Pastoriza, M. A. *Eur. Polym. J.* **2005**, *41*, 2793.
(19) Geoghegan, M. *Adv. Solid State Phys.* **2006**, *45*, 29.
(20) McKenna, G. B.; Flynn, K. M.; Chen, Y. H. *Macromolecules* **1989**, *22*, 4507.
(21) Treloar, L. R. G. *The Physics of Rubber Elasticity*, 3rd ed.; Clarendon Press: Oxford, U.K., 1975.
(22) Queslel, J. P. ; Mark, J. E. In *Comprehensive Polymer Science, 2, Polymer Properties*; Booth, C., Price, C., Eds.; Pergamon: Oxford, U.K., 1989, 271.
(23) Flory, P. J. *Priciples of Polymer Chemisry*; Cornell University Press: Ithaca, NY, 1953.
(24) Flory, P. J. *J. Chem. Phys.* **1941**, *9*, 660.
(25) Huggins, M. L. *J. Chem. Phys.* **1941**, *9*, 440.
(26) Valanis, K. C.; Landel, R. F. *J. Appl. Phys.* **1967**, *38*, 2997.
(27) McKenna, G. B.; Flynn, K. M.; Chen, Y. H. *Polym. Commun.* **1988**, *29*, 272.
(28) McKenna, G. B.; Flynn, K. M.; Chen, Y. H. *Polymer* **1990**, *31*, 1937.
(29) McKenna, G. B.; Hinkley, J. A. *Polymer* **1986**, *27*, 1368.
(30) McKenna, G. B.; Flynn, K. M.; Chen, Y. H. in *Molecular Basis of Polymer Networks*; Baumgartner, A., Picot, C.E., Eds.; Springer-Verlag: Berlin, 1989, 127.
(31) McKenna, G. B.; Horkay, F. *Polymer* **1994**, *35*, 5737.
(32) James, H. M.; Guth, E. *J. Chem. Phys.* **1943**, *11*, 455.
(33) James, H. M.; Guth, E. *J. Chem. Phys.* **1947**, *15*, 669.
(34) Flory, P. J. *J. Chem. Phys.* **1977**, *66*, 5720.
(35) Flory, P. J.; Erman, B. *Macromolecules* **1982**, *15*, 800.
(36) Han, W. H.; Horkay, F.; McKenna, G. B. *Math. Mech. Solids* **1999**, *4*, 139.
(37) Erman, B.; Monnerie, L. *Macromolecules* **1989**, *22*, 3342.
(38) Erman, B.; Monnerie, L. *Macromolecules* **1992**, *25*, 4465.
(39) Matlab by Mathworks, Inc. version R2011b (7.13.0.564)